

# Gauge-invariant condensation in the nonequilibrium quark-gluon plasma

Jürgen Berges,<sup>1</sup> Kirill Boguslavski,<sup>2,3</sup> Mark Mace,<sup>3,4</sup> and Jan M. Pawłowski<sup>1</sup>

<sup>1</sup>*Institute for Theoretical Physics, Heidelberg University, Philosophenweg 12, 69120 Germany*

<sup>2</sup>*Institute for Theoretical Physics, Technische Universität Wien, 1040 Vienna, Austria*

<sup>3</sup>*Department of Physics, University of Jyväskylä, P.O. Box 35, 40014, Jyväskylä, Finland*

<sup>4</sup>*Helsinki Institute of Physics, University of Helsinki, P.O. Box 64, 00014, Helsinki, Finland*

The large density of gluons, which is present shortly after a nuclear collision at very high energies, can lead to the formation of a condensate. We identify a gauge-invariant order parameter for condensation based on elementary non-perturbative excitations of the plasma, which are described by spatial Wilson loops. Using real-time lattice simulations, we demonstrate that a self-similar transport process towards low momenta builds up a macroscopic zero mode. Our findings reveal intriguing similarities to recent discoveries of condensation phenomena out of equilibrium in table-top experiments with ultracold Bose gases.

*Introduction.* In high-energy collider experiments with heavy nuclei, the far-from-equilibrium matter formed shortly after the collision is expected to have a high gluon density [1, 2]. It has been argued that this initial over-occupation of gluons may be so large that – if the system were in thermal equilibrium with same energy density – a condensate would be needed to account for the excess of gluons [3]. The possibilities for a condensate of gluon fields have been discussed in detail [4]. However, the subject was disputed in view of simulation results for the plasma’s evolution, which do not support Bose condensation of gluon fields [5–7]. The analysis is complicated by the fact that the underlying theory of quantum chromodynamics (QCD) is a gauge theory. Physical observables are gauge invariant, and examples of gauge-invariant operators for nonequilibrium condensation have been studied in the Abelian Higgs model [8].

In this work, we demonstrate that initial over-occupation of gluons leads to the formation of a gauge-invariant condensate. The definition of the latter takes into account that the infrared excitations of non-Abelian gauge theories are extended objects, which can be computed from Wilson loops [9–12]. Analyzing nonequilibrium spatial Wilson loops, we identify a transport process for these excitations towards low momenta that builds up a macroscopic zero mode. The time evolution is computed from classical-statistical lattice gauge theory simulations, which provide an accurate non-perturbative description in the over-occupied regime [6, 11, 13, 14]. We consider the non-expanding system following Refs. [9, 11, 12], which established for nonequilibrium spatial Wilson loops a self-similar area-law with a time-dependent spatial string tension.

We compare our results for the non-Abelian plasma with the far-from-equilibrium dynamics of Bose condensation for a scalar order-parameter field [15–17] and find remarkable similarities. The build-up of the scalar macroscopic zero mode is described in terms of a self-similar behavior with universal scaling exponents [16]. Table-top experiments with ultracold quantum gases now discovered these universal transport processes building up a condensate starting from initial over-occupation of

bosonic excitations of trapped atoms [18, 19]. Comparing the characteristic infrared scaling exponents of the Bose gas and the non-Abelian plasma, we observe an agreement within errors. This corroborates similar findings of universal scaling behavior in the perturbatively occupied regimes at higher momenta [5, 6, 20], where the plasma’s longitudinal expansion plays an important role [14, 21, 22].

*Self-similar attractor.* In high-energy nuclear collisions, the initially produced gluons are expected to have typical momenta of order the saturation scale  $Q_s$ , at time  $t \sim 1/Q_s$  [1, 2], where we use natural units with  $\hbar = c = 1$ . While the running gauge coupling  $\alpha_s(Q_s)$  is small for large enough  $Q_s$ , the system is strongly correlated because the gluon occupancies  $\sim 1/\alpha_s(Q_s)$  are large.

Here we consider the high-energy limit, because in this case the non-perturbative quantum problem can be mapped onto a classical-statistical lattice gauge theory, whose far-from-equilibrium evolution can be rigorously studied using large-scale computer simulations [13, 14]. The characteristic initial over-occupation is translated into energy density  $\sim Q_s^4/\alpha_s$  and fluctuations to initialize the lattice gauge theory evolution [5, 14, 21]. In the following, dimensionful quantities will be given in suitable powers of  $Q_s$ .

With such highly occupied initial conditions for low momenta  $p \lesssim Q_s$ , the system approaches a universal self-similar attractor after a transient time that is insensitive to the precise value of the coupling and to details of the initial conditions [5, 6, 12, 14, 21, 23–25]. It has been shown that a hierarchy of scales exists in the vicinity of this non-thermal fixed point, in analogy to the weakly-coupled equilibrium plasma at temperature  $T$  with the separation of scales of hard  $p \sim T$ , soft (Debye)  $p \sim gT$ , and ultrasoft (magnetic) momenta  $p \sim g^2T$  for  $g^2 = 4\pi\alpha_s \ll 1$ . The non-thermal fixed point is characterized by a hard momentum scale  $\Lambda(t)$  that dominates energy density and grows as  $\Lambda \sim t^{-\beta}$  with  $\beta = -1/7$  for the considered case of  $d = 3$  spatial dimensions without expansion. The typical occupation number at hard momenta decreases  $\sim t^{4\beta}$ , such that the energy density is

conserved and transported towards larger momenta. An intermediate scale is given by the Debye screening mass  $m_D \sim t^\beta$ , decreasing with time [5, 11, 14, 26, 27].

The dynamics becomes non-perturbative at the magnetic scale  $p_{\text{mag}}$ , which can be defined as the momentum scale where the occupancy is  $\simeq 1/\alpha_s$ . While initially all characteristic momentum scales are of the same order  $Q_s$ , during the self-similar evolution the occupation numbers decrease, which leads to the scale separation  $p_{\text{mag}} \ll m_D \ll \Lambda$ . As pointed out in Ref. [5], the evolution of the magnetic scale may be estimated approximately as  $p_{\text{mag}} \sim t^{-2/7}$  using the power-law form of the occupation number distribution extracted in the perturbative regime.

*Spatial Wilson loop out of equilibrium.* Focusing on dynamics at the magnetic scale, we consider the spatial Wilson loop as a gauge-invariant quantity that captures the long-distance behavior of gauge fields  $\mathcal{A}$ , defined as

$$W(\Delta x, \Delta y, t) = \frac{1}{N_c} \text{Tr} \mathcal{P} e^{-i g \int_{\mathcal{C}[\Delta x, \Delta y]} \mathcal{A}_i(\mathbf{z}, t) dz_i}, \quad (1)$$

where  $N_c$  is the number of colors of  $SU(N_c)$  gauge theory and the index  $i$  labels spatial components [28]. Here  $\mathcal{P}$  denotes path ordering, and the trace is in the fundamental representation. For simplicity, we consider rectangular paths  $\mathcal{C}[\Delta x, \Delta y]$  with lengths  $\Delta x = |\mathbf{x}_2 - \mathbf{x}_1|$  and  $\Delta y = |\mathbf{y}_2 - \mathbf{y}_1|$  with  $\mathbf{y}_1 \equiv \mathbf{x}_1$ , and area  $A = \Delta x \Delta y$  (cf. Fig. 1).

We will be interested in the expectation value of the spatial Wilson loop during the nonequilibrium evolution, which we denote by  $\langle W \rangle$ . More precisely, we define our spatial Wilson loop on an arbitrary plane on a  $d = 3$  dimensional cubic lattice. We consider only on-plane Wilson loops, however, it has been observed [11] that there is no difference within available statistics if one also includes off-plane Wilson loops. Expectation values are obtained from averages over classical-statistical runs with random initial seeds until convergence is observed. We also average over fixed area loops within a single random initial seed. The Wilson loop expectation value becomes then a function of the absolute values of the three-dimensional vectors  $\Delta \mathbf{x}$  and  $\Delta \mathbf{y}$ .

Self-similar scaling of the far-from-equilibrium Wilson loop has been established in Ref. [12]. Accordingly, the nonequilibrium dynamics in this regime is described by

$$\langle W(A, t) \rangle = \omega_S(A/t^\zeta) \quad (2)$$

in terms of a time-independent universal scaling exponent  $\zeta$  and scaling function  $\omega_S$ . Moreover, for large  $A/t^\zeta$  the scaling function obeys

$$\lim_{(A/t^\zeta) \rightarrow \infty} (-\log \omega_S(A/t^\zeta)) \sim A/t^\zeta. \quad (3)$$

This implies a time-dependent string tension  $\sigma(t) = -\partial \log \langle W \rangle / \partial A \sim t^{-\zeta}$ , which can be linked to the dynamics of topological configurations [11]. The scaling exponent  $\zeta$  for both  $SU(2)$  and  $SU(3)$  gauge theory was seen

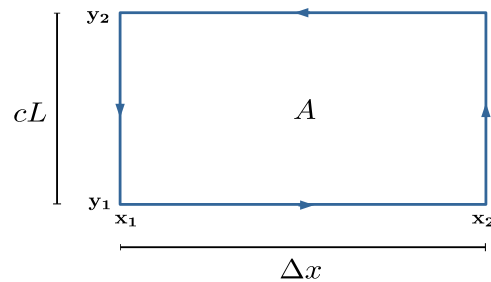


FIG. 1. Visualization of the rectangular path employed for  $\langle W(\Delta x, cL, t) \rangle$  with fixed length  $\Delta y = cL$  and  $c < 1$ .

to agree at the percent level [12], and we will perform our numerical simulations for  $SU(2)$ . The numerical values of the scaling exponent  $\zeta$  obtained in Refs. [11] and [12] differ slightly within errors, and we give improved estimates obtained at larger evolution times below in Eq. (9). Here, we note that the values of the scaling exponents for the ultra-soft scale  $\sqrt{\sigma}$  obtained from the lattice and the above perturbatively motivated estimate for  $p_{\text{mag}}$  are rather close, which suggests  $\sqrt{\sigma} \sim p_{\text{mag}}$ . This links the nonequilibrium spatial string tension to the magnetic scale, where the occupancy becomes non-perturbatively large. The positive value for  $\zeta$  signals evolution towards larger length scales, with characteristic area  $A(t) \sim t^\zeta$ .

*Gauge-invariant condensation far from equilibrium.* In order to study condensation, we propose to consider the closed Wilson line  $\langle W(\Delta x, cL, t) \rangle$  as a function of  $\Delta x$  with fixed length  $\Delta y = cL$  and real parameter  $c$ , as illustrated in Fig. 1. While  $L$  denotes the entire length of the lattice, its periodicity implies that the longest physical distance for  $\Delta y$  is  $L/2$ . Though all numerical results shown will employ  $c = 1/2$  accordingly, we explicitly checked that paths with  $c = 1/4$  and  $1/8$  lead to analogous results.

The employed closed spatial Wilson line as an order-parameter for condensation is reminiscent of the Polyakov line correlator [28–30]. The latter is the closed Wilson line in temporal direction, which is widely employed in thermal non-Abelian gauge theory. The Polyakov line correlator serves as an order parameter for the confinement-deconfinement phase transition at finite temperature [28–30]. Here, we employ the Wilson line in spatial direction for the description of ultra-soft momenta as motivated above.

Condensation is signaled by a macroscopic zero mode of  $\langle W(\Delta x, cL, t) \rangle$ , which is obtained by integrating with respect to  $\Delta x$  and dividing through the volume  $V_c = (cL)^d$  in the limit  $L \rightarrow \infty$ . We define the condensate

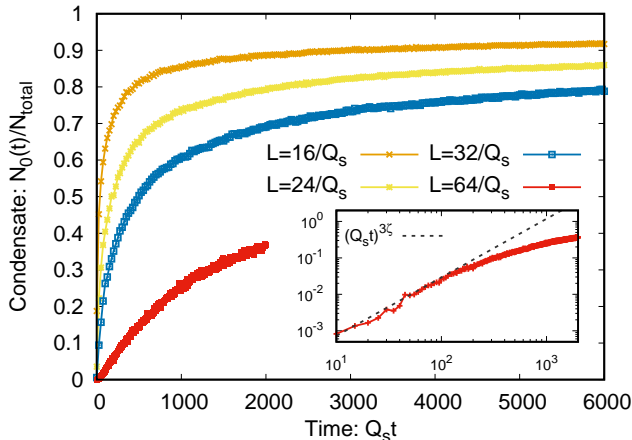


FIG. 2. Condensate fraction as a function of time for different volumes. Here  $c = 1/2$ ,  $\zeta = 0.54$ , and the lattice spacing  $Q_s a_s = 0.5$ . Inset: Logarithmic plot to demonstrate the early-time scaling of Eq. (6).

fraction for given  $L$  as

$$\begin{aligned} \frac{N_0(t, cL)}{N_{\text{total}}} &\equiv \frac{1}{V_c} \int_0^{cL} d^d \Delta x \langle W(\Delta x, cL, t) \rangle \\ &= \frac{1}{V_c} \int_0^{cL} d^d \Delta x \omega_S(\Delta x cL/t^\zeta) \\ &= \left( \frac{t^\zeta}{(cL)^2} \right)^d h((cL)^2/t^\zeta). \end{aligned} \quad (4)$$

For the second equality, we used the scaling behavior (2), and we define the function

$$h((cL)^2/t^\zeta) = \int_0^{(cL)^2/t^\zeta} d^d x \omega_S(x). \quad (5)$$

According to Eq. (4), in the scaling regime the condensate fraction is a function of the ratio  $(cL)^2/t^\zeta$  only. A first important case is when  $(cL)^2/t^\zeta$  is large. This characterizes the behavior of the condensate for large enough volumes at fixed time. If  $\omega_S$  is a rapidly decreasing function at large arguments, such as in Eq. (3), then Eq. (4) takes the form

$$\lim_{(cL)^2/t^\zeta \gg 1} \left( \frac{N_0(t, cL)}{N_{\text{total}}} \right) \simeq \left( \frac{t^\zeta}{(cL)^2} \right)^d h_\infty \quad (6)$$

with the asymptotic constant  $h_\infty = \lim_{x \rightarrow \infty} h(x)$ . Since  $\zeta$  is positive, Eq. (6) describes the growth of the condensate following a power-law in time. Once the entire volume becomes correlated, the condensate growth is expected to terminate, and is bounded by

$$\frac{N_0(t, cL)}{N_{\text{total}}} \leq 1, \quad (7)$$

since the Wilson loop satisfies  $W \leq 1$ .

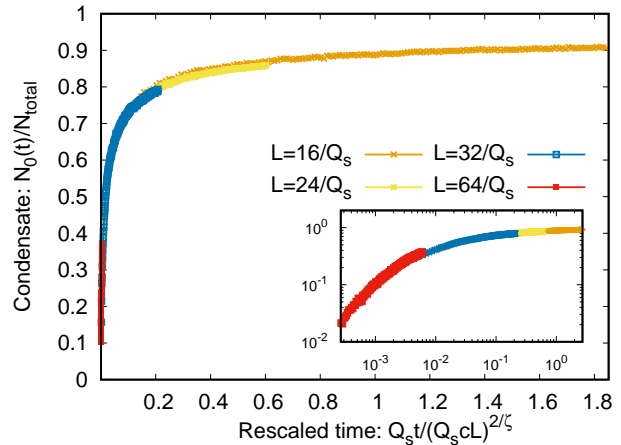


FIG. 3. Same as in Fig. 2 but as a function of rescaled time. All curves fall on top of each other showing the emergence of a macroscopic zero mode. Inset: Same curves on a logarithmic scale.

We verify the above parametric estimates by our lattice simulation data in  $d = 3$  spatial dimensions. The condensate fraction is shown in Fig. 2 as a function of time for different volumes with  $32^3$ ,  $48^3$ ,  $64^3$  and  $128^3$  lattice sites. The lattice spacing is  $a_s = 0.5$  in units of  $Q_s$ , and we have checked the insensitivity of our results to this choice. One observes that the zero mode indeed grows with time approaching a finite value. In the inset, the system with the largest volume reveals the power law growth of Eq. (6) at early times.

The scaling of the condensate formation time,  $t_{\text{cond}}$ , with volume can then be estimated by

$$t_{\text{cond}} \sim (cL)^{2/\zeta}. \quad (8)$$

As a consequence, according to Eq. (4) the evolution of the condensate fraction  $N_0(t, cL)/N_{\text{total}}$  is then only a function of the ratio  $t/t_{\text{cond}}$ . This is demonstrated in Fig. 3, where the same curves as in Fig. 2 are shown as functions of the rescaled time  $t/t_{\text{cond}}$  in linear and logarithmic scaling in the main panel and in the inset, respectively. All curves fall on top of each other, which signals the emergence of a macroscopic zero mode with the condensate fraction approaching  $N_0(t, cL)/N_{\text{total}} \simeq 0.92$  at the latest simulation times. Employing the  $\chi^2$ -procedure outlined in Ref. [14], we use this to extract

$$\zeta = 0.54 \pm 0.04 \text{ (stat.)} \pm 0.05 \text{ (sys.)}, \quad (9)$$

where systematic uncertainty results from variation of the length fraction  $c$ . This value for  $\zeta$  agrees within errors with the previously measured value using the self-similarity of Wilson loops [12], and from extracting the string tension [11].

*Comparison to Bose condensation of scalar fields.* We now compare our findings for the gauge theory to the theoretically and experimentally established condensation dynamics in ultracold Bose gases far from equilib-

rium [15, 16, 18]. Here we consider the example of an interacting Bose gas in three spatial dimensions described by a complex scalar order-parameter field  $\phi(t, \mathbf{x})$ . The s-wave scattering length  $a$  and density  $n = N_{\text{total}}^\phi/V$  of the Bose gas can be used to define a characteristic momentum scale  $Q = \sqrt{16\pi an}$ . In this setup,  $Q$  plays a similar role as the saturation scale for gluons in the gauge theory case, and the diluteness  $\sqrt{na^3}$  provides the dimensionless coupling parameter. In the dilute regime, where  $\sqrt{na^3} \ll 1$ , an over-occupied Bose gas features large occupancies  $\sim 1/\sqrt{na^3}$  for modes with momenta of order  $Q$ .

The nonequilibrium dynamics for scalars starting from over-occupation has been studied in great detail [15–17, 22, 31–38]. For spatially translation invariant systems, the infrared regime exhibits the self-similar scaling behavior

$$\frac{\langle \{\phi(t, \mathbf{x}_1), \phi^\dagger(t, \mathbf{x}_2)\} \rangle}{\langle \{\phi(t, 0), \phi^\dagger(t, 0)\} \rangle} = f_S(\Delta x/t^\beta). \quad (10)$$

Here  $\langle \{\phi, \phi^\dagger\} \rangle$  is the connected part of the anticommutator correlation and  $f_S$  denotes the scaling function, with scaling exponent [16, 17, 39]

$$\beta = 0.55 \pm 0.05. \quad (11)$$

The positive value for  $\beta$  signals evolution towards larger scales, with characteristic length  $\Delta x(t) \sim t^\beta$ . Accordingly, this corresponds to scaling towards low momentum modes in Fourier space. Asymptotically, the scaling function obeys [40]

$$\lim_{(\Delta x/t^\beta) \rightarrow \infty} (-\log f_S(\Delta x/t^\beta)) \sim \Delta x/t^\beta. \quad (12)$$

Using that  $N_{\text{total}}^\phi = \int_0^L d^d x \langle \{\phi(t, \mathbf{x}), \phi^\dagger(t, \mathbf{x})\} \rangle / 2 = V \langle \{\phi(t, 0), \phi^\dagger(t, 0)\} \rangle / 2$  is conserved in the non-relativistic system, the condensate fraction is

$$\begin{aligned} \frac{N_0^\phi(t)}{N_{\text{total}}^\phi} &= \frac{1}{V} \int_0^L d^d x \frac{\langle \{\phi(t, x), \phi^\dagger(t, 0)\} \rangle}{\langle \{\phi(t, 0), \phi^\dagger(t, 0)\} \rangle} \\ &= \frac{1}{V} \int_0^L d^d \Delta x f_S(\Delta x/t^\beta) \\ &= \left(\frac{t^\beta}{L}\right)^d h^\phi(L/t^\beta), \end{aligned} \quad (13)$$

with

$$h^\phi(L/t^\beta) = \int_0^{L/t^\beta} d^d x f_S(x). \quad (14)$$

Following along the lines of the discussion for the gauge theory, the condensation time for scalars then scales as

$$t_{\text{cond}} \sim L^{1/\beta}, \quad (15)$$

and the scalar system exhibits an early-time power law growth of the condensate fraction with  $t^{\beta d}/L^d$  for large volumes, subsequently approaching a finite value [16].

One observes that practically all of the above equations for scalars have precise corresponding expressions in the gauge theory, such as (13) replacing (4). Comparing these equations, there is an apparent difference concerning the  $L^2$ -dependence of the gauge theory expressions, whereas the corresponding ones for scalars depend on  $L$ . This additional power of  $L$  appears because we chose for the gauge theory  $\Delta y$  to scale with  $L$ . Instead, we could also assign a fixed extent to  $\Delta y$ . This does not change the condensation phenomenon we are reporting here, but will merely change the scaling with  $L$ . For instance, for fixed  $\Delta y$  the condensate formation time scales with the length as  $t_{\text{cond}}^{\Delta y = \text{const}} \sim (cL)^{1/\zeta}$  in complete analogy to (15), which we confirmed numerically for  $\Delta y = 8$ . Moreover, in both theories there is a corresponding conserved quantity. In the scalar case it is given by the conserved particle number density  $\sim \langle \{\phi(t, 0), \phi^\dagger(t, 0)\} \rangle$ , while in the gauge theory this role is played by  $\langle W(\Delta x = 0, cL, t) \rangle = \text{const}$ .

In view of this close correspondence, it is remarkable that even the values for the infrared scaling exponents  $\zeta$  in Eq. (9) and  $\beta$  in Eq. (11) agree well within errors. This is highly non-trivial, since we are comparing relativistic and non-relativistic systems with different symmetry groups and field content. However, though we have considered the example of a non-relativistic Bose gas, the same infrared scaling and condensation properties have been established for relativistic  $N$ -component real scalar field theories [16]. Even the anisotropic dynamics of relativistic scalars with longitudinal expansion along the  $z$ -direction, relevant in the context of heavy-ion collision kinematics, shows a very similar condensation behavior [41]. Apparent differences of the values of the scaling exponents result from geometrical differences associated to the dilution of the expanding system. Because of the strong enhancement in the over-occupied infrared regime, the low momentum modes exhibit essentially isotropic properties, such that the scaling function is again given by the isotropic  $f_S$  appearing in Eq. (10) also for the expanding case.

*Conclusions.* We have demonstrated that initial over-occupation in non-Abelian gauge theory at very high energies leads to the emergence of a macroscopic zero mode for the gauge-invariant closed spatial Wilson line. The condensate growth follows a power law at early times  $\sim (t/t_{\text{cond}})^{\zeta d}$  for large volumes, which terminates when the entire volume becomes correlated. The condensate formation time  $t_{\text{cond}} \sim (cL)^{2/\zeta}$  grows with system size. The scaling exponent  $\zeta$  is universal, such that its value is independent of the details of the underlying microscopic parameters like coupling strength or initial conditions.

Our comparison to theoretically and experimentally established condensation dynamics in scalar field theories uncovers an intriguing similarity in the infrared scaling behavior of non-Abelian gauge theory and (non-)relativistic scalars. Even the values for the universal scaling exponents agree within errors. In all these different theories, condensation arises from initial over-occupation as a consequence of a self-similar transport

process towards large distances in the presence of a conserved quantity. These robust ingredients can be found in a wide range of nonequilibrium systems from early-universe cosmology [31] to cold quantum gases [18, 19].

### ACKNOWLEDGMENTS

We thank S. Floerchinger, O. Garcia-Montero, A. Ipp, A. Kurkela, T. Lappi, A. Mazeliauskas, J. Peuron, A. Piñeiro Orioli, A. Rebhan, K. Reygers, S. Schlichting, R. Venugopalan for discussions and/or collaborations on

related work. The work is supported by EMMI, the BMBF grant 05P18VHFCA, and is part of and supported by the DFG Collaborative Research Centre SFB 1225 (ISOQUANT) as well as by the DFG under Germany's Excellence Strategy EXC - 2181/1 - 390900948 (the Heidelberg Excellence Cluster STRUCTURES). M.M. is supported by the European Research Council, grant ERC-2015-CoG-681707. This research used resources of the National Energy Research Scientific Computing Center (NERSC), a U.S. Department of Energy Office of Science User Facility operated under Contract No. DE-AC02-05CH11231.

- 
- [1] F. Gelis, E. Iancu, J. Jalilian-Marian, and R. Venugopalan, *Ann. Rev. Nucl. Part. Sci.* **60**, 463 (2010).
- [2] T. Lappi and L. McLerran, *Nucl. Phys.* **A772**, 200 (2006).
- [3] J.-P. Blaizot, F. Gelis, J.-F. Liao, L. McLerran, and R. Venugopalan, *Nucl. Phys.* **A873**, 68 (2012).
- [4] S. Floerchinger and C. Wetterich, *JHEP* **03**, 121 (2014).
- [5] A. Kurkela and G. D. Moore, *Phys. Rev.* **D86**, 056008 (2012).
- [6] M. C. Abraao York, A. Kurkela, E. Lu, and G. D. Moore, *Phys. Rev.* **D89**, 074036 (2014).
- [7] J.-P. Blaizot, J. Liao, and Y. Mehtar-Tani, *Nucl. Phys.* **A961**, 37 (2017).
- [8] T. Gasenzer, L. McLerran, J. M. Pawłowski, and D. Sexty, *Nucl. Phys.* **A930**, 163 (2014).
- [9] J. Berges, S. Scheffler, and D. Sexty, *Phys. Rev.* **D77**, 034504 (2008).
- [10] A. Dumitru, T. Lappi, and Y. Nara, *Phys. Lett.* **B734**, 7 (2014).
- [11] M. Mace, S. Schlichting, and R. Venugopalan, *Phys. Rev.* **D93**, 074036 (2016).
- [12] J. Berges, M. Mace, and S. Schlichting, *Phys. Rev. Lett.* **118**, 192005 (2017).
- [13] G. Aarts and J. Berges, *Phys. Rev. Lett.* **88**, 041603 (2002).
- [14] J. Berges, K. Boguslavski, S. Schlichting, and R. Venugopalan, *Phys. Rev.* **D89**, 114007 (2014).
- [15] J. Berges and D. Sexty, *Phys. Rev. Lett.* **108**, 161601 (2012).
- [16] A. Piñeiro Orioli, K. Boguslavski, and J. Berges, *Phys. Rev.* **D92**, 025041 (2015).
- [17] I. Chantesana, A. Piñeiro Orioli, and T. Gasenzer, *Phys. Rev.* **A99**, 043620 (2019).
- [18] M. Prüfer, P. Kunkel, H. Strobelt, S. Lannig, D. Linneemann, C.-M. Schmied, J. Berges, T. Gasenzer, and M. K. Oberthaler, *Nature* **563**, 217 (2018).
- [19] S. Erne, R. Bücke, T. Gasenzer, J. Berges, and J. Schmiedmayer, *Nature* **563**, 225 (2018).
- [20] S. Schlichting, *Phys. Rev.* **D86**, 065008 (2012).
- [21] J. Berges, K. Boguslavski, S. Schlichting, and R. Venugopalan, *Phys. Rev.* **D89**, 074011 (2014).
- [22] J. Berges, K. Boguslavski, S. Schlichting, and R. Venugopalan, *Phys. Rev. Lett.* **114**, 061601 (2015).
- [23] J. Berges, S. Scheffler, and D. Sexty, *Phys. Lett.* **B681**, 362 (2009).
- [24] A. Kurkela and G. D. Moore, *JHEP* **12**, 044 (2011).
- [25] K. Boguslavski, A. Kurkela, T. Lappi, and J. Peuron, (2019), arXiv:1907.05892 [hep-ph].
- [26] T. Lappi and J. Peuron, *Phys. Rev.* **D95**, 014025 (2017).
- [27] K. Boguslavski, A. Kurkela, T. Lappi, and J. Peuron, *Phys. Rev.* **D98**, 014006 (2018).
- [28] I. Montvay and G. Münster, *Quantum fields on a lattice*, Cambridge Monographs on Mathematical Physics (Cambridge University Press, 1997).
- [29] C. Gattringer and C. B. Lang, *Lect. Notes Phys.* **788**, 1 (2010).
- [30] H. J. Rothe, *World Sci. Lect. Notes Phys.* **43**, 1 (1992).
- [31] J. Berges, A. Rothkopf, and J. Schmidt, *Phys. Rev. Lett.* **101**, 041603 (2008).
- [32] C. Scheppach, J. Berges, and T. Gasenzer, *Phys. Rev.* **A81**, 033611 (2010).
- [33] J. Berges and D. Sexty, *Phys. Rev.* **D83**, 085004 (2011).
- [34] B. Nowak, D. Sexty, and T. Gasenzer, *Phys. Rev.* **B84**, 020506 (2011).
- [35] B. Nowak, J. Schole, D. Sexty, and T. Gasenzer, *Phys. Rev.* **A85**, 043627 (2012).
- [36] G. D. Moore, *Phys. Rev.* **D93**, 065043 (2016).
- [37] R. Walz, K. Boguslavski, and J. Berges, *Phys. Rev.* **D97**, 116011 (2018).
- [38] J. Deng, S. Schlichting, R. Venugopalan, and Q. Wang, *Phys. Rev.* **A97**, 053606 (2018).
- [39] A. Schachner, A. Piñeiro Orioli, and J. Berges, *Phys. Rev.* **A95**, 053605 (2017).
- [40] A. N. Mikheev, C.-M. Schmied, and T. Gasenzer, *Phys. Rev.* **A99**, 063622 (2019).
- [41] J. Berges, K. Boguslavski, S. Schlichting, and R. Venugopalan, *Phys. Rev.* **D92**, 096006 (2015).